

Structure Preserving Finite Volume Approximation of Cross-Diffusion Systems Coupled by a Free Interface

Clément Cancès¹, Jean Cauvin-Vila², Claire Chainais-Hillairet¹, and Virginie Ehrlacher²

¹ Univ. Lille, CNRS, Inria, UMR 8524 - Laboratoire Paul Painlevé, F-59000 Lille, France

² CERMICS (ENPC) & INRIA, Paris

Abstract. We propose a two-point flux approximation finite-volume scheme for the approximation of two cross-diffusion systems coupled by a free interface to account for vapor deposition. The moving interface is addressed with a cut-cell approach, where the mesh is locally deformed around the interface. The scheme preserves the structure of the continuous system, namely: mass conservation, nonnegativity, volume-filling constraints and decay of the free energy. Numerical results illustrate the properties of the scheme.

Keywords: cross-diffusion system, cut-cell method, finite volume scheme, free energy dissipation, moving interface, vapor deposition

1 A Free Interface Cross-Diffusion Model

We address a toy model to describe a physical vapor deposition process used for the fabrication of thin film layers [3]. We consider the evolving domain

$$\Omega(t) = (0, X(t)) \cup (X(t), 1), \quad t > 0,$$

where $\mathbb{R}_+ \ni t \rightarrow X(t) \in [0, 1]$ is the free interface between the solid (left) and the gas (right). Traces and jumps at the interface are respectively denoted by $f^s, f^g, [[f]] = f^g - f^s$. We consider n different chemical species represented by their densities of molar concentration $\mathbf{c} = (c_1, \dots, c_n)^T$. The local conservation of matter reads:

$$\partial_t \mathbf{c} + \partial_x \mathbf{J} = 0, \quad t > 0, \quad x \in \Omega(t), \quad (1a)$$

for some molar fluxes $\mathbf{J} := (J_1, \dots, J_n)^T$. Cross-diffusion phenomena are modelled differently in each phase. In the solid phase, the fluxes are given by

$$J_i = \sum_{j=1}^n \kappa_{ij}^s (c_j \partial_x c_i - c_i \partial_x c_j), \quad \text{in } (0, X), \quad i \in \{1, \dots, n\}, \quad (1b)$$

with cross-diffusion coefficients $\kappa_{ij}^s = \kappa_{ji}^s > 0$, which rewrites more compactly

$$\mathbf{J} = -\mathbf{A}_s(\mathbf{c}) \partial_x \mathbf{c}, \quad \text{in } (0, X), \quad (1c)$$

with a linear diffusion matrix $\mathbf{A}_s(\mathbf{c})$ (see [1]). In the gaseous phase, the fluxes are defined implicitly via the Maxwell-Stefan linear system (see [2])

$$\mathbf{A}_g(\mathbf{c})\mathbf{J} = -\partial_x \mathbf{c}, \text{ and } \sum_{i=1}^n J_i = 0, \text{ in } (X, 1), \quad (1d)$$

where $\mathbf{A}_g(\mathbf{c})$ is identical to $\mathbf{A}_s(\mathbf{c})$, except for possibly different cross-diffusion coefficients $\kappa_{ij}^g = \kappa_{ji}^g > 0$. The system is completed with an initial condition (\mathbf{c}^0, X^0) , no-flux conditions on the fixed boundary and the following conditions across the moving interface:

$$\mathbf{J}^s(t) - X'(t)\mathbf{c}^s(t) = \mathbf{F}(t) = \mathbf{J}^g(t) - X'(t)\mathbf{c}^g(t), \quad t > 0, \quad (1e)$$

where \mathbf{F} accounts for reaction mechanisms [6,7] and is defined, for some constant reference chemical potentials $\mu_i^{*,s}, \mu_i^{*,g} \in \mathbb{R}$, by the Butler-Volmer formulas: for $i \in \{1, \dots, n\}$,

$$\begin{aligned} F_i &= c_i^s \exp\left(\frac{\mu_i^{*,g} - \mu_i^{*,s}}{2}\right) - c_i^g \exp\left(\frac{\mu_i^{*,s} - \mu_i^{*,g}}{2}\right), \\ &= 2\sqrt{c_i^s c_i^g} \sinh\left(-\frac{1}{2}[\log(c_i) - \mu_i^*]\right). \end{aligned} \quad (1f)$$

Finally, the interface evolves according to

$$X'(t) = -\sum_{i=1}^n F_i, \quad (1g)$$

The system enjoys several important properties we aim at preserving at the discrete level: first, mass conservation follows from the local conservation (1a), no-flux conditions on the fixed boundary and the conservative condition (1e). Second, the system preserves the nonnegativity of the concentrations and the volume-filling constraints $\sum_{i=1}^n c_i = 1$ (satisfied by the initial condition), and we refer to such a solution as *admissible*. Finally, the functional

$$\mathcal{H}(\mathbf{c}, X) = \int_0^X h_s(\mathbf{c}) + \int_X^1 h_g(\mathbf{c}), \quad (2)$$

with density $h_\alpha(\mathbf{c}) = \sum_{i=1}^n c_i(\log(c_i) - \mu_i^{*,\alpha}) - c_i + 1$, for $\alpha \in \{s, g\}$, can be shown to satisfy, for some positive semi-definite mobility matrices $\mathbf{M}_s, \mathbf{M}_g$, the free energy dissipation relation [4,5]

$$\begin{aligned} \frac{d}{dt} \mathcal{H}(\mathbf{c}(t), X(t)) &= -\int_0^{X(t)} \partial_x \log(\mathbf{c})^T \mathbf{M}_s(\mathbf{c}) \partial_x \log(\mathbf{c}) \\ &\quad - \int_{X(t)}^1 \partial_x \log(\mathbf{c})^T \mathbf{M}_g(\mathbf{c}) \partial_x \log(\mathbf{c}) + \mathbf{F}(t)^T [[\log(\mathbf{c}) - \boldsymbol{\mu}^*]] \leq 0. \end{aligned} \quad (3)$$

One deduces from the dissipation inequality that stationary solutions (\bar{c}, \bar{X}) must be constant in (each connected part of) $\bar{\Omega} = (0, \bar{X}) \cup (\bar{X}, 1)$ and moreover, if $\bar{X} \in (0, 1)$, $F_i(\bar{c}_i^s, \bar{c}_i^g) = 0$ should hold. We characterize in [3] the stationary states of (1), as partially stated in Proposition 1.

Proposition 1 (Stationary states). Define the coefficients $\beta_i = \frac{e^{\mu_i^{*,g}}}{e^{\mu_i^{*,s}}}$, and let $m_i^0 = m_i^{0,s} + m_i^{0,g} > 0$ be the initial amount of each species in the system. Then there exists a (unique) two-phase stationary solution (i.e. such that $\bar{X} \in (0, 1)$) if and only if

$$\sum_{i=1}^n m_i^0 \beta_i > 1 \text{ and } \sum_{i=1}^n m_i^0 \frac{1}{\beta_i} > 1, \quad (4)$$

Moreover, the stationary state is explicitly computable from \bar{X} , which is itself solution to a convex nonlinear scalar equation.

2 Finite Volume Scheme

We consider $N \in \mathbb{N}^*$ reference cells of uniform size $\Delta x = \frac{1}{N}$. The $N + 1$ edge vertices are denoted by $0 = x_{\frac{1}{2}}, x_{\frac{3}{2}}, \dots, x_{N+\frac{1}{2}} = 1$. We consider a time horizon $T > 0$ and a time discretization with mesh parameter Δt defined such that $N_T \Delta t = T$ with $N_T \in \mathbb{N}^*$. The concentrations are discretized as $\mathbf{c}_{\Delta x}^p = (c_{i,K}^p)_{i \in \{1, \dots, n\}, K \in \{1, \dots, N\}}$ for $p \in \{0, \dots, N_T\}$. The interface is discretized as X^p for $p \in \{0, \dots, N_T\}$, and we denote by $x_{K^p+\frac{1}{2}} \in [0, 1]$ the closest vertex to X^p (the left vertex in case of equality). The mesh is locally modified around X^p : the cells K^p and $K^p + 1$ are deformed, as presented in Figure 1, where we denote by K the interface cell to alleviate the notations (this notation is used in all figures in this section). To account for this deformation, we introduce Δ_K^{p-1} the size of cell K at discrete time $t^{p-1} = (p-1)\Delta t$:

$$\Delta_K^{p-1} = \begin{cases} (X^{p-1} - x_{K^{p-1}-\frac{1}{2}}) & \text{if } K = K^{p-1}, \\ (x_{K^{p-1}+\frac{3}{2}} - X^{p-1}) & \text{if } K = K^{p-1} + 1, \\ \Delta x & \text{otherwise.} \end{cases} \quad (5)$$

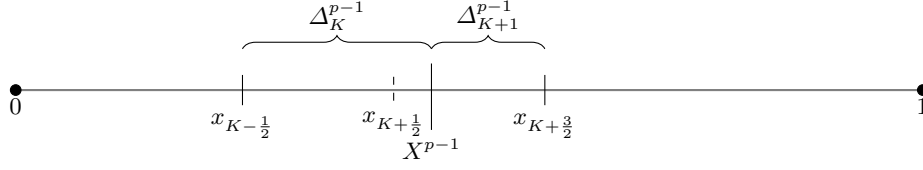
With this notation, the initial concentrations $\mathbf{c}^0 \in L^\infty(\Omega_0; \mathbb{A})$ are naturally discretized as $c_{i,K}^0 = \frac{1}{\Delta_K^0} \int_K c_i^0 dx$. Starting from the knowledge of $\mathbf{c}_{\Delta x}^{p-1}, X^{p-1}$, our scheme consists in

- i) solving the conservation laws and updating the interface position, leading to $\mathbf{c}_{\Delta x}^{p-\frac{1}{2}}, X^p$.
- ii) updating the mesh to Δ_K^p and post-processing the interface concentrations into the final values $\mathbf{c}_{\Delta x}^p$.

2.1 Conservation laws

The conservation laws (1a) are discretized implicitly as, for $K \in \{1, \dots, N\}, i \in \{1, \dots, n\}$,

$$\frac{1}{\Delta t} (\Delta_K^{p-\frac{1}{2}} c_{i,K}^{p-\frac{1}{2}} - \Delta_K^{p-1} c_{i,K}^{p-1}) + J_{i,x_{K+\frac{1}{2}}}^{p-\frac{1}{2}} - J_{i,x_{K-\frac{1}{2}}}^{p-\frac{1}{2}} = 0. \quad (6a)$$

Fig. 1: Mesh deformation at time $t^{p-1} = (p-1)\Delta t$.

where we have introduced the intermediate quantity (see Figure 2)

$$\Delta_K^{p-\frac{1}{2}} = \begin{cases} (X^p - x_{K^{p-1}-\frac{1}{2}}) & \text{if } K = K^{p-1}, \\ (x_{K^{p-1}+\frac{3}{2}} - X^p) & \text{if } K = K^{p-1} + 1, \\ \Delta x & \text{otherwise.} \end{cases} \quad (6b)$$

As for the numerical fluxes, the bulk fluxes (1b)-(1d) are discretized according to

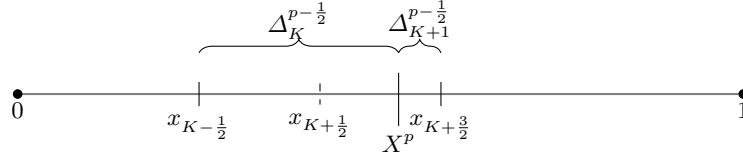


Fig. 2: Intermediate mesh deformation.

[4] in the solid phase and to [5] in the gaseous phase, in a way that preserves the bulk part of the dissipation structure (3). The interface fluxes (1f) are discretized as

$$J_{i,x_{K^{p-1}+\frac{1}{2}}}^{p-\frac{1}{2}} = F_i^{p-\frac{1}{2}} = c_{i,K^{p-1}}^{p-\frac{1}{2}} \exp\left(\frac{\mu_i^{*,g} - \mu_i^{*,s}}{2}\right) - c_{i,(K^{p-1}+1)}^{p-\frac{1}{2}} \exp\left(\frac{\mu_i^{*,s} - \mu_i^{*,g}}{2}\right). \quad (6c)$$

Finally, (1g) is discretized as

$$X^p = X^{p-1} - \Delta t \sum_{i=1}^n F_i^{p-\frac{1}{2}} \quad (6d)$$

We denote the solution to (6) by $(c_{\Delta x}^{p-\frac{1}{2}}, X^p)$.

2.2 Post-processing

When X^p crosses the center of a cell, one needs to update the interface cell from K^{p-1} to K^p and to adjust the concentrations accordingly. First, we can

derive a linear CFL condition from (6d) to bound $|X^p - X^{p-1}|$, so that we can enforce $|K^p - K^{p-1}| \leq 1$. If $K^p = K^{p-1}$, then we can directly iterate the scheme with $c_{\Delta x}^p = c_{\Delta x}^{p-\frac{1}{2}}$. Otherwise, let us illustrate the case of a right displacement $K^p = K^{p-1} + 1$ and let us use again the notation $K := K^{p-1}$ for simplicity. We perform the following steps (see Figure 3)

- i) *Projection*: The value $c_{i,K}^{p-\frac{1}{2}}$ is assigned to the virtual cell $(x_{K-\frac{1}{2}}, X^p)$. We assign this value to both the fixed cell $K = (x_{K-\frac{1}{2}}, x_{K+\frac{3}{2}})$ and the new interface cell $(K+1) = (x_{K+\frac{1}{2}}, X^p)$:

$$c_{i,K}^p = c_{i,K+1}^p = c_{i,K}^{p-\frac{1}{2}}. \quad (7)$$

- ii) *Average*: X^p replaces x_{K+1} as the interface node. We average the value in the cell $(K+2) = (X^p, x_{K+2})$:

$$c_{i,K+2}^p = \frac{1}{\Delta x + \Delta_{K+1}^{p-\frac{1}{2}}} \left[\Delta_{K+1}^{p-\frac{1}{2}} c_{i,K+1}^{p-\frac{1}{2}} + \Delta x c_{i,K+2}^{p-\frac{1}{2}} \right]. \quad (8)$$

- iii) In all other cells, $c_{i,K}^p = c_{i,K}^{p-\frac{1}{2}}$.

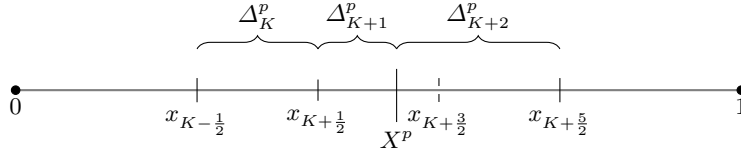


Fig. 3: Mesh deformation at time $t^p = p\Delta t$. $(K+1)$ is the new interface cell.

2.3 Numerical analysis

Let us introduce the discrete version of the free energy functional (2):

$$\mathcal{H}(c_{\Delta x}^p, X^p) = \sum_{i=1}^n \sum_{K \leq K^p} \Delta_K^p h^s(c_{i,K}^p) + \sum_{i=1}^n \sum_{K \geq K^p+1} \Delta_K^p h^g(c_{i,K}^p). \quad (9)$$

Proposition 2 gives some a priori estimates fulfilled by a solution to the scheme, leading to existence of a solution.

Proposition 2 (Structure preservation). *Given an admissible solution $(c_{\Delta x}^{p-1}, X^{p-1})$, there exists an admissible solution $(c_{\Delta x}^p, X^p)$ to the scheme (6).*

Moreover, the amount of matter of each species is conserved and a discrete version of the dissipation relation (3) is satisfied:

$$\begin{aligned} \mathbf{c}_{\Delta x}^p \geq 0, \text{ and } \sum_{i=1}^n c_{i,K}^p &= 1, \quad K \in \{1, \dots, N\}, \\ \sum_{K=1}^N \Delta_K^p c_{i,K}^p &= m_i^0, \quad i \in \{1, \dots, n\}, \\ \mathcal{H}(\mathbf{c}_{\Delta x}^p, X^p) &\leq \mathcal{H}(\mathbf{c}_{\Delta x}^{p-1}, X^{p-1}). \end{aligned}$$

We sketch some ingredients of the proof below, see [3] for details.

Proof. Concerning conservation of matter, it follows from summing the conservation laws (6a) over the cells K and the fact that the fluxes are conservative that, for any $i \in \{1, \dots, n\}$,

$$\sum_{K=1}^N \Delta_K^{p-\frac{1}{2}} c_{i,K}^{p-\frac{1}{2}} = \sum_{K=1}^N \Delta_K^{p-1} c_{i,K}^{p-1}.$$

If $K^p = K^{p-1}$, the result follows immediately. Otherwise, let us assume that $K^p = K^{p-1} + 1$. Then, setting $K = K^{p-1}$, it suffices to consider the three interface cells $K, K+1, K+2$ (see Figures 2 and 3). The result follows by definition of the post-processing formulas (7)-(8).

The proof of the nonnegativity of the concentrations and of the dissipation of the free energy follow the same lines that in [4,5]. For nonnegativity, one should reason by contradiction and use the sign of the fluxes when considering a cell where a nonpositive minimum is attained. For dissipation, the continuous dissipative structure of the interface fluxes (1f) is directly translated at the discrete level, provided one can define $\log(c_{i,K}^p)$.

The volume-filling constraints are proved by summing the conservation laws (6a) over i and noticing that (6d) can be rewritten

$$\sum_{i=1}^n F_i^{p-\frac{1}{2}} = -\frac{1}{\Delta t} \left(\Delta_{K^{p-1}}^{p-\frac{1}{2}} - \Delta_{K^{p-1}}^{p-1} \right),$$

so that one obtains a classical heat equation scheme on the quantity $\sum_{i=1}^n c_{i,K}^p$, as in [4,5].

Finally the existence proof follows from a topological degree argument.

3 Numerical Results

The numerical scheme has been implemented in the Julia language. The non-linear system is solved with Newton method, with stopping criterion $\|\mathbf{c}_{\Delta x}^{p,k+1} - \mathbf{c}_{\Delta x}^{p,k}\|_{\infty} \leq 10^{-12}$. Jacobians are efficiently automatically computed thanks to the ForwardDiff and SparseDiffTools packages.

Let us introduce a test case: we fix an initial interface $X^0 = 0.51$ and smooth initial concentrations $c_1^0(x) = c_2^0(x) = \frac{1}{4}(1 + \cos(\pi x))$, $c_3^0(x) = \frac{1}{2}(1 - \cos(\pi x))$ that will be suitably discretized. The cross-diffusion coefficients are taken equal in each phase, with values $\kappa_{12} = \kappa_{21} = 0.2$, $\kappa_{23} = \kappa_{32} = 0.1$, $\kappa_{13} = \kappa_{31} = 1$ (diagonal coefficients do not play any role). The reference chemical potential $\boldsymbol{\mu}^{*,s}, \boldsymbol{\mu}^{*,g}$ are given by $e^{\boldsymbol{\mu}^{*,s}} = [0.2 \ 0.4 \ 0.4]$, $e^{\boldsymbol{\mu}^{*,g}} = [1.2 \ 0.1 \ 0.1]$, so as to fulfill the equilibrium condition (4).

We illustrate the properties of the scheme on a uniform mesh of $N = 100$ cells with time step $\Delta t_1 = 6 \times 10^{-4}$ and a final time $T_1 = 5$. Snapshots of the simulation are presented in Figure 4, where one notices the formation and propagation of a discontinuity at the free interface. We also study the long-time asymptotics: we first compute accurately the stationary solution $(\mathbf{c}^\infty, X^\infty)$ obtained in Proposition 1. Then we study the relative free energy $\mathcal{H}(\mathbf{c}_{\Delta x}^p, X^p) - \mathcal{H}(\mathbf{c}^\infty, X^\infty)$ and relative interface $X^\infty - X^p$ over time. The results are given in Figure 5a, indicating exponential speed of convergence and monotonicity of both functionals. In particular, our scheme is well-balanced and preserves the asymptotics of the continuous system.

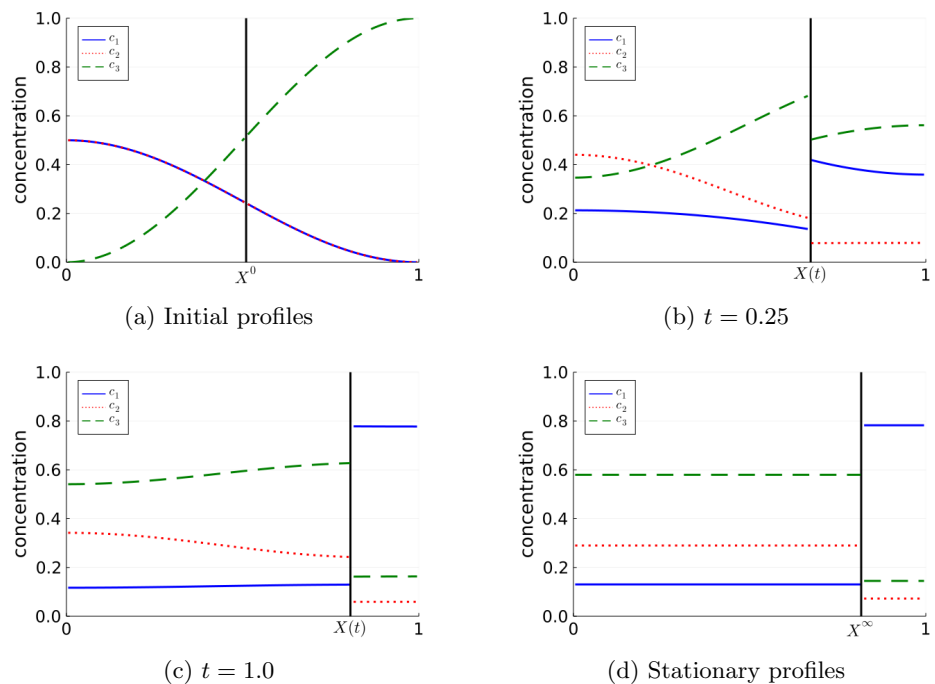


Fig. 4: Concentration profiles at different times.

Our second test is devoted to a convergence analysis with respect to the size of the mesh. We consider a fixed time step $\Delta t_2 = 10^{-4}$, a final time $T_2 = 0.25$,

uniform meshes from 2^3 to 2^{10} cells and we compare the different solutions with respect to a reference solution computed on a finer grid of 2^{11} cells. The space-time (resp. time) L^1 error on the concentrations (resp. on the interface) are displayed in Figure 5b. One clearly observes convergence, at first order in space for the concentrations. These results should be compared with the second order accurate one-phase schemes [4,5]. On the one hand, it is plausible that the interface treatment induces the loss of order. On the other hand, the discrete $L^1((0, 1))$ space distance we use to compare solutions is not perfectly adapted since the solutions are defined in slightly different domains. Rescaling all quantities might offer more insights into the convergence properties.

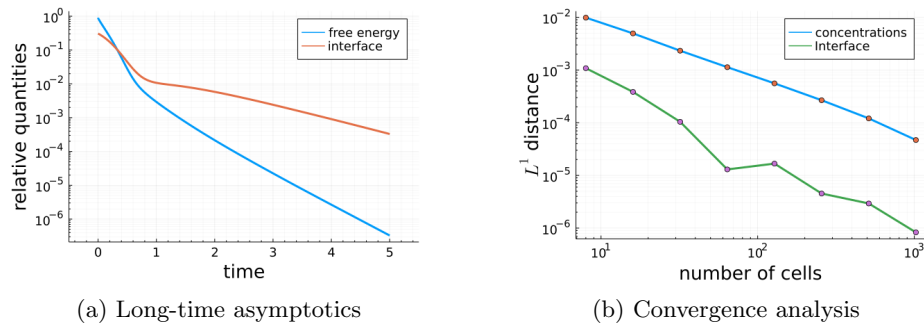


Fig. 5: $(\mathcal{H}(\mathbf{c}(t), X(t)) - \mathcal{H}(\mathbf{c}^\infty, X^\infty))$ and $(X^\infty - X(t))$ as functions of time (left). Convergence analysis of the solution under space grid refinement (right).

Acknowledgment The authors acknowledge support from the ANR project COMODO (ANR-19-CE46-0002) which funds the Ph.D. of Jean Cauvin-Vila.

References

1. Bakhta, A., Ehrlicher, V.: Cross-diffusion systems with non-zero flux and moving boundary conditions. *ESAIM:M2AN*, 52(4), pp.1385–1415 (2018).
2. Bothe D.: On the Maxwell-Stefan Approach to Multicomponent Diffusion. *Parabolic problems*, vol. 80, pp. 81-93 (2011).
3. Cancès, C., Cauvin-Vila, J., Chainais-Hillairet, C., Ehrlicher, V.: A Convergent Finite Volume Scheme for a Free Interface Cross-Diffusion Model. In preparation.
4. Cancès, C., Gaudeul, B.: A Convergent Entropy Diminishing Finite Volume Scheme for a Cross-Diffusion System. *SINUM*, 58(5), pp. 2684-2710 (2020).
5. Cancès, C., Ehrlicher, V., Monasse L.: Finite Volumes for the Stefan-Maxwell Cross-Diffusion System. *arXiv:2007.09951* (2020).
6. Glitzky A., Mielke A.: A gradient structure for systems coupling reaction–diffusion effects in bulk and interfaces. *ZAMP*, vol. 64, pp. 29-52 (2013).
7. Mielke, A., Peletier, M. A., Renger, D. M.: On the relation between gradient flows and the large-deviation principle, with applications to Markov chains and diffusion. *Potential Analysis*, 41, pp. 1293-1327 (2014).